



Triple Benefits of Cardanol as Chain Stopper, Flame Retardant and Reactive Diluent for Greener Alkyd Coating

Maxinne Denis, Cédric Totée, Damien Le Borgne, Rodolphe Sonnier, Sylvain Caillol, Claire Negrell

► To cite this version:

Maxinne Denis, Cédric Totée, Damien Le Borgne, Rodolphe Sonnier, Sylvain Caillol, et al.. Triple Benefits of Cardanol as Chain Stopper, Flame Retardant and Reactive Diluent for Greener Alkyd Coating. *Organics*, 2023, 4 (1), pp.109 - 125. 10.3390/org4010009 . hal-04037375

HAL Id: hal-04037375

<https://hal.science/hal-04037375>

Submitted on 20 Mar 2023

HAL is a multi-disciplinary open access archive for the deposit and dissemination of scientific research documents, whether they are published or not. The documents may come from teaching and research institutions in France or abroad, or from public or private research centers.

L'archive ouverte pluridisciplinaire **HAL**, est destinée au dépôt et à la diffusion de documents scientifiques de niveau recherche, publiés ou non, émanant des établissements d'enseignement et de recherche français ou étrangers, des laboratoires publics ou privés.

Article

Triple Benefits of Cardanol as Chain Stopper, Flame Retardant and Reactive Diluent for Greener Alkyd Coating

Maxinne Denis ^{1,2}, Cédric Totée ¹, Damien Le Borgne ², Rodolphe Sonnier ³, Sylvain Caillol ¹ and Claire Negrell ^{1,*}

¹ ICGM, University of Montpellier, CNRS, ENSCM, 34296 Montpellier, France

² Lixol, Groupe Berkem, 20 Rue Jean Duvert, 33290 Blanquefort, France

³ Polymers Composites and Hybrids (PCH), IMT Mines Alès, 30319 Alès, France

* Correspondence: claire.negrell@enscm.fr

Abstract: Cardanol, a waste from the food industry and widely produced (1 Mt/y), has been used as a chain stopper during the polycondensation of short oil alkyd resins in order to replace benzoic acid. Then, phosphorylated cardanol has been added in order to both reduce solvent content and bring flame-retardant (FR) properties to the alkyd resins. The renewable carbon content of the formulations has been increased up to 23%. The impact of the introduction of phosphorylated cardanol molecules on the drying time and flexibility has been studied as well as the thermal and flame-retardant properties by differential scanning calorimeter, thermogravimetric analysis and pyrolysis-combustion flow calorimeter. The most effective flame-retardant coating that was associated with excellent FR properties and excellent coating properties has been obtained with phosphate-cardanol added at 2%wt of P. Indeed, the film properties were closed to the classical alkyd resin, the solvent content was reduced by 50% and the pHRR decreased by 42% compared to the reference alkyd resin.

Keywords: alkyd resins; cardanol; reactive diluent; flame retardant; coatings



Citation: Denis, M.; Totée, C.; Le Borgne, D.; Sonnier, R.; Caillol, S.; Negrell, C. Triple Benefits of Cardanol as Chain Stopper, Flame Retardant and Reactive Diluent for Greener Alkyd Coating. *Organics* **2023**, *4*, 109–125. <https://doi.org/10.3390/org4010009>

Academic Editor: Tomasz K. Olszewski

Received: 23 December 2022

Revised: 21 February 2023

Accepted: 9 March 2023

Published: 15 March 2023



Copyright: © 2023 by the authors. Licensee MDPI, Basel, Switzerland. This article is an open access article distributed under the terms and conditions of the Creative Commons Attribution (CC BY) license (<https://creativecommons.org/licenses/by/4.0/>).

1. Introduction

Alkyd resins (AR) are polyesters modified with unsaturated fatty chains, obtained by step growth polymerization between fatty acids and/or vegetable oils, anhydrides and/or acids, and polyols [1–3]. They have been synthetized for the first time by Kienle in the mid-1920s and industrialized in the 1930s by General Motors [4–6]. They can be classified into three categories according to their oil length [7–9], which is defined as the mass percentage of fatty chains on the total mass of the AR. Long oil ARs contain at least 60 wt% of oil, whereas medium oil resins length contain between 40 and 60 wt% of oil [10,11]. The last class is short oil ARs that contain less than 40 wt% of oil. Short oil ARs exhibit the highest molar masses due to their lowest content of fatty acids, a mono-functional monomer that can act as a chain stopper [12]. Therefore, benzoic acid, a petrosourced mono-functional monomer, is generally used as chain stopper for the synthesis of short oil ARs. Hulsbosch et al. have synthetized a novel AR with pyroglutamic acid, an amino acid, to replace benzoic acid [13]. Nevertheless, the molar mass, viscosity and thermal stability of ARs containing amino acids were relatively low compared to commercial ARs. Koning et al. also used mono-functional amino acids (glycine or phenylalanine-derived monosuccinimides) to replace benzoic acid in ARs synthesis to enhance biobased content [14]. The authors demonstrated that ARs modified with these amino acids show faster drying, increased hardness but also a darker color. However, the high price of amino acids is a limiting factor for their use in the synthesis of ARs. More recently, our group has successfully synthetized novel ARs based on mono- and di-functional cardanol monomers [15]. Cardanol-modified ARs have demonstrated better thermal stability than conventional ARs while maintaining other film properties (drying

time, adhesion, flexibility and gloss). The introduction of 25% of mono-functional cardanol allowed for replacing benzoic acid in polycondensation of ARs. The results of this study highlighted the valorization of a waste from the food industry produced in large amounts (1 Mt/y) [16].

Moreover, to reduce their viscosity and allow their application as a coating, these short ARs can contain up to 50% of solvent. Solvents, such as xylene or White Spirit, have a boiling point below 250 °C at atmospheric pressure, so they can be considered as volatile organic compounds (VOC) whose presence is limited by recent regulations [17–19]. Hence, an effective approach to reduce the VOC content of alkyd coating formulations is the use of reactive diluents (RD). These allow for reducing the viscosity of the formulation and then react with the binder during curing and therefore cannot leach out of the coating [20,21]. RD need to exhibit a low viscosity and volatility, a great compatibility to promote solubility and reactive functions to have the capacity to react with the binder (ARs) during the drying process by oxidative reactions [22–25]. Several researchers studied the advantages of modified cardanol as reactive diluent for AR. Wang et al. studied the impact of cardanol (CO), cardanol methacrylate (MACO) and triethoxysilane-functionalized cardanol (TSCO), introduced as RD [26]. The results have demonstrated that the viscosity of AR decreased with the increasing amount of these cardanol derivatives. Hence, the introduction of 5 wt% MACO or TSCO reduced the amount of solvent (around 9 wt%) for an equivalent final viscosity of the AR formulations [27].

Due to their high contents of carbon and hydrogen elements, ARs suffer from flammability. One way to compensate for this limitation is the addition of flame retardant (FR) in the polymer matrix. Nowadays, because of environmental concerns, the development of halogen-free flame-retardants has gained increasing attention. Phosphorus-based flame retardants are one of the most promising alternatives to halogen flame retardants to protect polymers from combustion. Another recent study of our group focused on the synthesis of novel phosphorylated cardanol introduced as flame retardant and reactive diluent in ARs [28]. The best result was combined excellent flame-retardant properties (a reduction of 41% of the heat release rate compared to the reference AR) and the conservation of film properties of conventional AR. Nevertheless, this study used short oil ARs synthetized with benzoic acid. A new approach could allow a complete valorization of cardanol by introducing it for polycondensation of ARs as well as for the post functionalization to form covalent bonds during the crosslinking reaction (Figure 1). This approach could overcome the three main limitations of short oil ARs: petrosourced monomers, high content of VOC and flammability. Hence, phosphorylated cardanol reactive (PO_xCR) diluents were synthetized and introduced in AR formulations in order to reduce the amount of VOC. The crosslinking of ARs was investigated by high resolution magic angle spinning (HRMAS) nuclear magnetic resonance (NMR) and Fourier transform infrared (FT-IR). The viscosity of the AR was analyzed by rheology. The flame-retardant properties were investigated by thermogravimetric analysis (TGA), pyrolysis combustion flow calorimeter analysis (PCFC) and cone calorimeter. ARs were applied as coatings on wood supports for the cone calorimeter analysis. Furthermore, gloss, hardness, chemical resistance, corrosion resistance and drying time were studied on each coating.

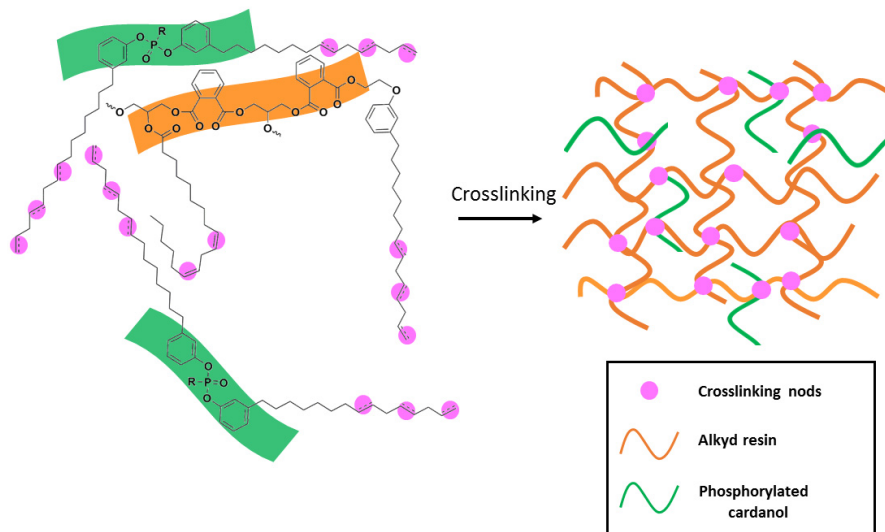


Figure 1. General scheme of crosslinking cordanol-modified alkyd resin containing phosphorylated cardanol ($R = \text{OPh} (\text{PO}_4\text{CR})$ or $\text{Ph} (\text{PO}_3\text{CR})$).

2. Materials and Methods

(1) Materials

Tall oil fatty acid (TOFA), glycerol, phthalic anhydride and mix of driers (a solution containing cobalt octoate, calcium octoate and zirconium octoate) were kindly supplied by Lixol (Groupe Berkem, Blanquefort, France). Cardanol NX-2026 was kindly provided by Cardolite. Phenylphosphonic dichloride, phenyl dichlorophosphate, triethylamine (TEA), xylene, p-toluenesulfonic acid (pTSA), sulfuric acid (H_2SO_4), sodium bicarbonate (NaHCO_3), ethylene carbonate and 1,5-diazabicyclo[4.3.0]non-5-ene (DBN) were purchased from Sigma Aldrich, St. Louis, MI, USA. Sodium chloride (NaCl), sodium bicarbonate (NaHCO_3), hydrochloric acid (HCl), magnesium sulfate (MgSO_4), dichloromethane (DCM) and tetrahydrofuran (THF) were purchased from VWR International S.A.S (Fontenay-sous-Bois, France). The NMR solvents used were CDCl_3 and THF-d_8 from Eurisotop. All reagents were used as received.

(2) Characterizations

Nuclear Magnetic Resonance

NMR samples were prepared with CDCl_3 as solvent and the analyses were performed using a Bruker Avance 400 MHz spectrometer at 25 °C. The structure of monomers was determined by hydrogen nuclear magnetic resonance (^1H NMR), and phosphorus nuclear magnetic resonance (^{31}P NMR). The ^1H NMR spectra were recorded at 8 kHz for spectral width, 3 kHz for transmitter frequency offset and 4 s for acquisition. Eight scans were performed. Quantitative conditions were obtained with a 30° pulse (3 μs) and a relaxation delay at 1 s. The ^{31}P NMR spectra were recorded at 64 kHz for spectral width, 8000 Hz for transmitter frequency offset and 1 s for acquisition time. Four scans were performed. Quantitative conditions were obtained with a 30° pulse (2.7 μs) and a relaxation delay at 20 s. External references were trimethylsilane (TMS) for ^1H and phosphoric acid (H_3PO_4) for ^{31}P NMR. Shifts were given in ppm. Furthermore, to confirm the crosslinking of cardanol-modified ARs, high resolution magic angle spinning (HRMAS) NMR experiments have been investigated. HRMAS NMR experiments were carried out on a Varian VNMRS 600 MHz spectrometer equipped with a wide bore magnet ($B_0 = 14.1$ T). Prior to ^1H HRMAS NMR experiments, cured ARs were grinded thanks to a cryogenic grinder and the powders were injected into a 4 mm quartz zirconia HRMAS rotor. Then, THF-d_8 was injected as solvent and experiments were performed at 20 °C, 9.6 kHz for spectral width, 1200 Hz for transmitter frequency offset and 1.7 s for acquisition time. Eight scans were performed. Quantitative conditions were obtained with a 30° pulse (3.9 μs) and a relaxation delay at 1 s.

Acid values (AV)

Acid values were determined according to the ISO 2114 standard. It is the mass of potassium hydroxide (KOH) in milligrams that is required to neutralize one gram of AR. Approximatively 1 g of the reaction mixture was withdrawn and solubilized in a neutralizing solution (80/20 xylene/ethanol). The solution was then titrated with a KOH solution at 0.1 mol·mL⁻¹. Thanks to the following Equation (1), the acid value was calculated.

$$AV = \frac{V_{KOH} \times M_{KOH} \times C_{KOH}}{m \times N.V.C.} \quad (1)$$

AV: Acid value; *V_{KOH}*: volume of KOH solution introduced to neutralize the alkyd resin (mL); *M_{KOH}*: molecular weight of KOH (g·mol⁻¹); *C_{KOH}*: concentration of KOH (mol·mL⁻¹); *m*: mass of alkyd resin withdraw (g); *N.V.C.*: Non Volatile Content.

Renewable carbon content

The renewable carbon content (%rC) has been calculated using the Equations (2)–(4), where *N_{TOFA}* corresponds to the number of renewable carbons in TOFA (around 18). *N_{CARDANOL}* corresponds to the number of renewable carbons for the monofunctional cardanol (21). The *N_{GLYCEROL}* corresponds to the number of renewable carbons in glycerol (3). The *N_{CARDANOL}* corresponds to the total carbon number in the monofunctional cardanol (24). The *N_{TOFA}* and the *N_{GLYCEROL}* correspond to the total number of carbons in TOFA (18) and glycerol (3), respectively. The *N_{PA}* and the *N_{BA}* correspond to the non-renewable carbons of the phthalic anhydride (8). The *N_{PoXCR}* corresponds to the non-renewable carbons of phenylphosphonic dichloride or phenyl dichlorophosphate (6).

$$\%rC_{alkyd\ resin} = \frac{n_{TOFA} \times N_{TOFA} + n_{CARDANOL} \times N_{CARDANOL} + n_{GLYCEROL} \times N_{GLYCEROL}}{n_{TOFA} \times N_{TOFA} + n_{CARDANOL} \times N_{CARDANOL} + n_{GLYCEROL} \times N_{GLYCEROL} + n_{PA} \times N_{PA} + n_{BA} \times N_{BA}} \quad (2)$$

$$\%rC_{Phosphorylated\ cardanol} = \frac{n_{cardanol} \times N_{cardanol}}{n_{CARDANOL} \times N_{CARDANOL} + n_{PoXCR} \times N_{PoXCR}} \quad (3)$$

%rC Formulation

$$\begin{aligned} &= \%rC_{alkyd\ resin} \times wt\%_{alkyd\ resin} \\ &+ \%rC_{phosphorylated\ cardanol} \times wt\%_{phosphorylated\ cardanol} \\ &+ wt\%_{solvent\ (xylene)} \end{aligned} \quad (4)$$

Measurement of ¹⁴C

The measurement of ¹⁴C was performed by CIRAM laboratory. The sample undergoes combustion at 920 °C and is transformed into gas. During this stage, a first verification of the C/N ratio was carried out using an elemental analyzer (Elementar Vario ISOTOPE Select). The residual carbon dioxide (CO₂) was separated from the other combustion residues using a zeolite trap. Then, this carbon dioxide is transformed into graphite using an automated system (AGE 3, Ion Plus) by catalysis. At the same time, the ¹³C/¹²C (expressed as δ¹³C) and ¹⁵N/¹⁴N (expressed as δ¹⁵N) ratios were measured on a mass spectrometer dedicated to the measurement of stable isotope ratios, with an error less than 0.1 ‰ (IRMS, Elementar Isoprime precisION). The different isotopes of carbon are separated by mass spectrometry, with a 250 kV accelerator in joint venture with JSC Barnas (ISO 9001 and ISO 14001). Then, the ¹⁴C concentration is determined by simultaneously comparing the measurements of ¹⁴C, ¹³C and ¹²C with those contained in reference products (oxalic acid, CO₂ standard, coal). The conventional carbon-14 age was calculated using the method described by Stuiver and Polach. It takes into account the correction of isotopic fractionation (δ¹³C), based on the comparison ¹³C/¹²C and ¹⁴C/¹²C concentration ratios. This factor makes it possible to control the effects of possible pollution and to assess the reliability of the measurement. This is a good indicator of the “quality” of the sample. The precision of the pMC measurement is presented at 1σ (1 sigma relative to the uncertainty). International standards NIST

4990C, IAEA-C-7 and IAEA-C-9 were used. $\delta^{13}\text{C}$ is expressed in per thousand (‰) relative to the international standard V-PDB (Vienna Pee Dee Belemnite). $\delta^{15}\text{N}$ is expressed in permille (‰) relative to air. The international standards IAEA-600, IAEA-N-2 and BCR-657 were used.

Rheological analyses

Rheological analyses were performed on a ThermoScientific Haake Mars 60 rheometer equipped with a 35-mm-cone-plate geometry. The analyses were performed at 20 °C with a shear rate of 10 s⁻¹. All the resins were compared at the non-volatile content of 60 wt%.

Size-exclusion chromatography (SEC)

Molecular weights of ARs were determined by size-exclusion chromatography (SEC). SEC was recorded using a triple-detection GPC from Agilent Technologies (Santa Clara, CA, USA) with its corresponding Agilent software, dedicated to multidetector GPC calculation. The system used two PL1113-6300 ResiPore 300 × 7.5 mm columns with THF as the eluent with a flow rate of 1 mL min⁻¹. The detector was a 390-LC PL0390-0601 refractive index detector. The entire SEC system was thermostated at 35 °C. Polymethylmethacrylate (PMMA) standards were used for calibration between 540 and 2,210,000 g·mol⁻¹. The typical sample concentration was 15 mg·mL⁻¹.

Fourier Transform Infrared Spectroscopy

The Fourier transform infrared (FTIR) spectra were acquired on a Thermo Scientific Nicolet iS50 FT-IR equipped with an attenuated total reflectance cell (ATR). The data were analyzed using the software OMNIC Series 8.2 from Thermo Scientific (Waltham, MA, USA).

Gel content

The resins were mixed with 5 wt% of mix of driers (cobalt octoate, calcium octoate and zirconium octoate) in order to accelerate the autoxidative process. Then, films were obtained thanks to a film applicator. All the dry films exhibited a thickness of 60 µm. Three samples from the same AR films, of around 20 mg each, were separately immersed in THF for 24 h. The three samples were then dried in a ventilated oven at 80 °C for 24 h. The gel content (GC) was calculated using Equation (5), where m₂ is the mass of the dried material and m₁ is the initial mass. Reported gel content are average values of the three samples.

$$\text{GC} = \frac{m_2}{m_1} \times 100 \quad (5)$$

Differential scanning calorimetry

Differential scanning calorimetry (DSC) analyses were carried out using a NETZSCH DSC200F3 calorimeter. The calibration was performed using adamantane, biphenyl, indium, tin, bismuth and zinc standards. Nitrogen was used as the purge gas. The thermal properties were analyzed at 20 °C/min between –100 and 100 °C to observe the glass transition temperature.

Thermogravimetric analyses

Thermogravimetric analyses (TGA) of the cured ARs were carried out to determine the thermal stability and were performed on a Netzsch TG 209F1 apparatus under 40 mL·min⁻¹ nitrogen flow. The protective gas used was nitrogen with a 20 mL·min⁻¹ flow. Approximately 10–12 mg of sample was placed in an alumina crucible and heated from room temperature to 850 °C with a 20 °C·min⁻¹ heating rate.

Pyrolysis combustion flow calorimeter analysis

Flammability of resins was analyzed using a pyrolysis combustion flow calorimeter (PCFC). About 3–4 mg were placed in the pyrolyzer, undergoing an increase in temperature from 20 °C to 750 °C at a rate of 1 °C·s⁻¹ under a nitrogen flow. Pyrolytic gases were sent

to a combustor heated at 900 °C under air flow ($N_2/O_2 = 80/20$). At this temperature and with 20% oxygen, combustion was considered to be complete. Heat release rate (HRR) was determined according to oxygen depletion (Huggett's relation) as the cone calorimeter test. PCFC analyses correspond to anaerobic pyrolysis followed by high temperature oxidation of decomposition products (complete combustion) [29]. All samples were tested in triplicate.

Cone calorimeter test

Cone calorimeter was used to investigate the fire behavior of resins used as coating on wood specimens. The ARs were applied on a pine wood sample ($100 \times 100 \times 25$ mm), with a density of $500 \text{ kg} \cdot \text{m}^{-3}$, in order to obtain a coating of $0.01 \text{ g} \cdot \text{cm}^{-2}$. The samples were placed at 2.5 cm below a conic heater and isolated by rock wool. The samples were exposed to a $35 \text{ kW} \cdot \text{m}^{-2}$ heat flux in well-ventilated conditions (air rate $24 \text{ L} \cdot \text{s}^{-1}$) in the presence of a spark igniter to force the ignition. Heat release rate (HRR) was determined by oxygen depletion according to Huggett principle (1 kg of consumed oxygen corresponds to 13.1 MJ of heat released) [30]. Peak of Heat Release Rate (pHRR) is the maximal value of the heat release rate. The total heat released (THR) was obtained by integration of HRR curves. All samples were tested in triplicate.

Film properties

100 μm wet films were applied with a film applicator and dried at 25 °C under a relative humidity of 30%. The thickness of dry films was 60 μm in all cases. Adhesion was measured on an aluminum plate using a cross-cut tester of 1 mm BYK, according to ISO 2409:2020 standard. The method is explained in Supporting Information (SI). The hardness (Persoz hardness) was determined according to ISO 1522:2006 standard with a TQC SP0500 pendulum hardness tester (method explained in Supplementary Materials). Gloss was measured based on ISO 2813:2014 standard and the measurements were performed on substrates at 60° and 20° using a TQC Polygloss (method explained in Supplementary Information). The color of the ARs was determined using the Gardner color scale (explained in Supplementary Information). The values for the hardness and the gloss measurements were determined at day +10 (D+10) after the application of the film. The drying time of the resins was taken as the time required to obtain a tack-free film. The chemical resistance of the ARs was studied on water (H_2O), hydrochloric acid (HCl), sodium hydroxide (NaOH) and sodium chloride (NaCl) [31]. Approximatively 10 ± 1 mg of the cured ARs were immersed inside each solvent for 6 hours at room temperature and stirred at 200 rpm. Then, they were dried in an oven at 80 °C for 12 h. The residual mass percentage (wt% residue) was determined using Equation (6). The analyses were made in triplicate for each sample and the reported residual masses percentage are average values of the three samples.

$$\text{wt\% residue} = \frac{m_2}{m_1} \times 100 \quad (6)$$

m_1 : mass of the alkyd resin sample before being immersed in solvent; m_2 : mass of the alkyd resin sample after being immersed in a solvent and dried in an oven.

Complementary information is available in the Supplementary Material.

(3) Synthesis

Mono-functional cardanol (EC), phosphonate-cardanol (PO_3CR) and phosphate-cardanol (PO_4CR) were synthetized following the previously published procedure by Denis et al. and the structures are presented in Figure 2 [15,28].

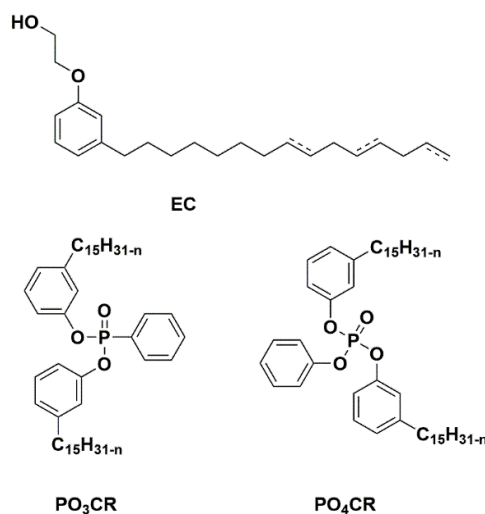


Figure 2. Structures of EC, PO₃CR and PO₄CR molecules.

2.1. Synthesis of Mono-Functional Cardanol (EC) Containing Alkyd Resin

A short oil alkyd resin containing tall oil fatty acids (TOFA) and ethoxy cardanol (EC) was synthetized by a solvent process also using glycerol and phthalic anhydride. In a reactor equipped with a mechanical stirrer, 0.06 mol of EC, 0.18 mol of TOFA and 0.430 mol of glycerol were firstly added. Then, 0.46 mol of phthalic anhydride was introduced when the reaction reached 200 °C. Reaction mixture was heated to 220 °C using xylene as azeotropic solvent to remove water. The reaction was continued until an acid value inferior to 15 mg of KOH/g of resin was obtained. The resins have 38 wt% of fatty acids in their composition, which is why they can be classified as short oil length. The stoichiometry of f_{OH}/f_{COOH} for all AR was 1.23.

2.2. Preparation of the Formulation

Different ratios of phosphorylated cardanol derivatives were added to obtain AR with 0 wt%, 1 wt% and 2 wt% of phosphorus. The different compositions are shown in Table 1.

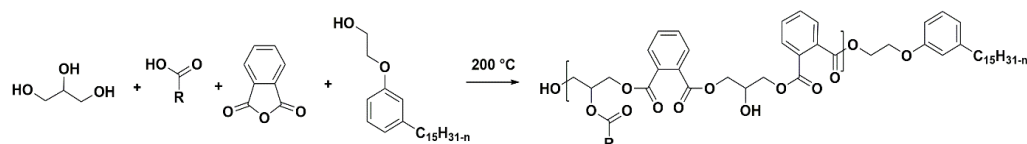
Table 1. Compositions of alkyd resins with PO_xCR at the same viscosity (5.6 Pa·s).

	Reference	Phosphonate		Phosphate	
wt% P	0	1	2	1	2
Xylene content (wt%)	40	30	20	30	20
Reactive diluent content (wt%)	0	15	37	15	39
Alkyd resin content (wt%)	60	55	43	54	41
N.V.C. (wt%)	60	70	80	70	80

3. Results and Discussion

3.1. Synthesis of Cardanol-Modified Alkyd Resins

The AR has been synthetized through a fatty acid process with the presence of a low amount of xylene as an azeotropic solvent (Scheme 1). The presence of xylene is necessary to allow the extraction of water during the synthesis.



Scheme 1. General synthesis of EC alkyd resin.

The final acid value (AV) was 12. It corresponds to the free acids groups in the resins. The final AV must be between 10 and 15 for a short oil AR. An AV lower than 10 could

lead to the gelation of the AR [31], whereas an AV higher could lead to hydrolysis, for example. The resin is classified as short oil length, before formulation, because it contains 38 wt% of fatty acids. Moreover, this AR exhibits a renewable carbon content (*rC%*) of 58 *rC%* and the PO_xCR compounds exhibit a *rC%* of 88%. The introduction of such reactive diluent allowed for increasing the renewable carbon content (*rC%*) of the ARs as presented in Table 2. Indeed, the reference AR exhibited a value of 35% of renewable carbon content in the final formulation, whereas it was 58 *rC%* for the AR with 2 wt% P from PO₄CR. Moreover, the *rC%* values calculated theoretically or measured with the AMS radiocarbon method (EN 16640:2017) exhibited similar results. Thereby, the calculation method developed in this study made it possible to obtain results similar to those obtained using a standardized method.

Table 2. Viscosity, T_g and gel content of phosphorylated cardanol reactive diluent alkyd resins with a fixed NVC at 60 wt%.

	Reference	Phosphonate	Phosphate	
wt% P	0	1	2	1
η (Pa·s) (xylene: 40 wt%)	5.6	1.5	0.2	1.6
<i>rC%</i> of formulations	35	45	57	45
<i>rC%</i> (EN 16640:2017) *	37	48	50	53
T_g (°C)	19	5	-5	6
Gel content (%)	94 ± 1	92 ± 1	90 ± 2	92 ± 2
			91 ± 1	

* Those *rC%* values were obtained thanks to the AMS radiocarbon method at the CIRAM laboratory.

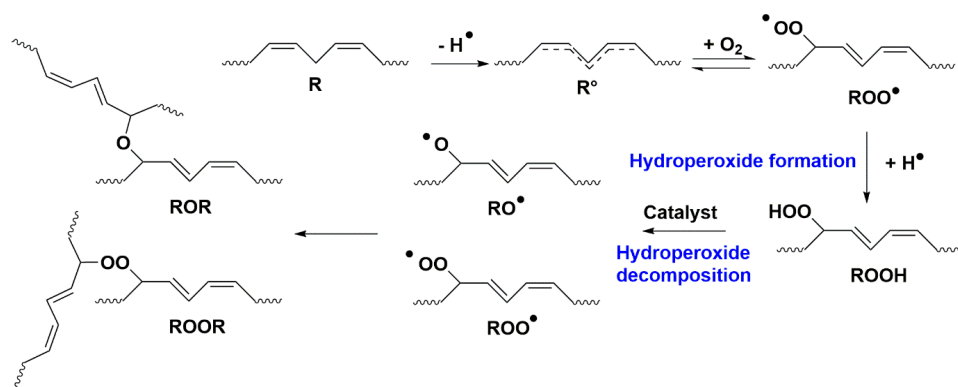
Furthermore, a recent study synthesized biobased phthalic anhydride, derived from furan compound that may further increase the renewable carbon content [32].

Size exclusion chromatography (SEC) allowed for determining the weight average molecular weight M_w of the resin (PMMA equivalent) at 150,000 g·mol⁻¹. High molecular weights are characteristic of short oil ARs since the molecules are more compact, rigid and have less fatty acid (monofunctional) side chain in the polymer linkages [12,33].

A minimal amount of 10 wt% of xylene was required to obtain a homogenous solution. Nevertheless, this study focused on the maximal reduction in solvent content to reduce the VOC of the final ARs while maintaining good film properties. Thus, according to the results obtained in our previous study, the minimal xylene content has been set at 20 wt% [28]. The PO_xCR diluents were introduced with different phosphorus percentages (1 and 2 wt% of phosphorus) in the reference AR. The amount of xylene was calculated to target a viscosity close to 5 Pa·s for all the resins, such as the one of the reference AR (Table 1). Then, the non-volatile content (NVC) was evaluated. The growing amount of PO_xCR diluents introduced in the reference AR allowed for reducing the solvent to target the same viscosity at ±0.2 Pa·s for all the AR formulations. The increased amount of PO_xCR diluent introduced allowed for decreasing the quantity of AR, which can also reduce the viscosity. The introduction of 2 wt% of phosphorus (2 wt% P) with PO_xCR diluents allowed for reducing the amount of solvent by 20 wt% compared to the reference AR, which corresponds overall to a 50% reduction in VOC.

Then, to do a correct comparison between all the formulations, the viscosities of all the resins were also compared with the same non-volatile content of 60 wt%, as presented in Table 2. First, the introduction of 1 wt% P, which represents 15 wt% of PO₃CR and PO₄CR diluents, reduced the viscosity by 73% compared to the reference EC alkyd resin. With a phosphorus percentage of 2 wt% P, the viscosity decreased to 0.2 Pa·s.

During the curing of the formulation, the phosphorylated diluents were crosslinked to AR, thanks to the introduction of a low percentage of a drier (mix of metallic salts). Indeed, cardanol and AR are both composed of unsaturated chains, which allow oxidative curing in air [34]. Autoxidation of alkyds is a three-stage process including peroxidation, peroxide decomposition, and cross-linking reaction that occurs by a free-radical mechanism. (Scheme 2).



Scheme 2. Oxidative drying alkyd mechanism.

To confirm the presence of a crosslinked network, analyses were made such as the determination of the gel content (GC) and the investigation of the disappearance of the chemical shift of unsaturations ($C=C$) by ^1H HRMAS NMR and FTIR. The gel content was defined as the mass of insoluble material after being exposed for 24 h in THF. Indeed, an insoluble 3D network is formed when the AR is cured. For all the ARs, the GC was higher than 90%, confirming the crosslinking (Table 2). To confirm crosslinking of ARs, ^1H HRMAS experiments (Figures S6–S10) were also performed. Indeed, ARs should crosslink with phosphorylated cardanol through the $C=C$ double bond. The two peaks at 5.15 and 5.95 ppm could be attributed to the three protons of the terminal double bonds and the peak at 5.45 ppm could be attributed to the protons of internal double bonds. In SI Figures S1–S5, the peaks of the protons of terminal double bonds (H_i and H_g) disappeared. This result could be explained by the difference of reactivity between the protons of the terminal double bonds and the protons of internal double bonds. Indeed, the terminal double bonds protons are more reactive than the ones of internal double bonds in the alkyl chains. The integrations of the peaks of the double also demonstrated a decrease by 50% for the cardanol-modified ARs compared to the reference AR. Those results were consistent with the ones obtained from the GC analysis. Then, FTIR analyses demonstrated the curing of AR through the $C=C$ of alkyl chains of cardanol [31]. Indeed, the disappearance of the characteristic peak of olefinic C-H of cardanol at 3003 cm^{-1} in all the AR films containing cardanol is shown in Figure 3a,b. This last result confirmed the crosslinking of AR through the $C=C$ of cardanol.

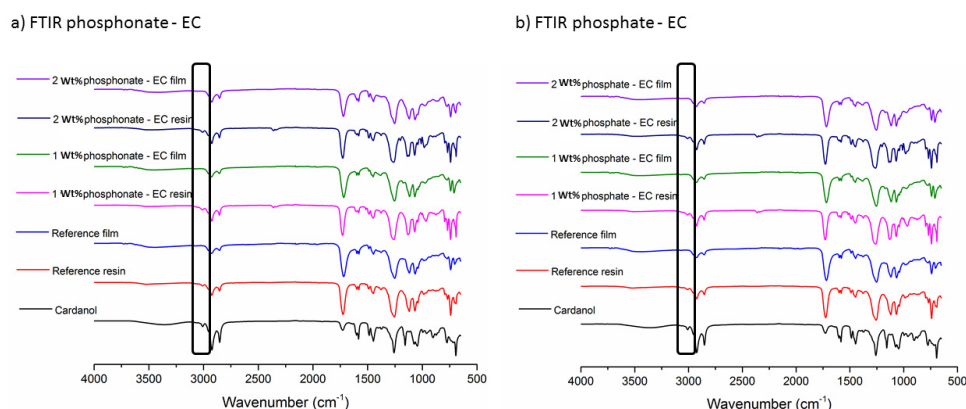


Figure 3. FTIR spectra of cardanol, alkyd resins and alkyd resin films with (a) PO_3CR and (b) PO_4CR .

Differential scanning calorimetry (DSC) analyses were carried out to determine the glass transition temperature (T_g) of curing films and are summarized in Table 2. The flexible alkyl chain and bulky phenyl groups of PO_xCR diluents may impact the physical properties of the resins compared to the use of xylene. Indeed, xylene is removed from the film during the drying step, whereas PO_xCR are crosslinked with the AR during the drying step. The

PO_xCR -free resin exhibited a T_g value of 19 °C, while the introduction of PO_xCR diluent (causing the diminution of the AR content) reduced the T_g values of modified ARs. Indeed, for ARs containing phosphonate-cardanol, T_g values ranged from 5 °C for the AR with 1 wt% P to -5 °C for the AR with 2 wt% P. This evolution was mainly due to the introduction of dangling cardanol chains provided by PO_xCR diluent, which improved flexibility and reduced T_g . In this study, the T_g were lower than the T_g of our previous study for the same formulations containing PO_xCR diluent.²⁸ This could be due to benzoic acid contained in previous ARs as a chain stopper, which is more rigid than ethoxy cardanol with fatty chains.

Moreover, the reduction in the T_g could also be attributed to the reduction in AR content while the amount of PO_xCR was increasing. The T_g values were not impacted by the oxydation state of phosphorus. The T_g of 2 wt% P ARs were, respectively, -5 °C for both PO_3CR and PO_4CR . The T_g could impact the application of ARs. Some surfaces, such as wood, require flexible coatings whereas metal requires harder coatings.

3.2. Thermal and Flame-Retardant Properties

Thermal and flame-retardant properties were investigated in this part to highlight the influence of the PO_xCR diluents in ARs. The thermal decomposition of all AR films were investigated by thermogravimetric analyses (TGA) under nitrogen flow (i.e., anaerobic pyrolysis). Figure 4 shows the thermograms of the neat EC AR, and with, respectively, 1 wt% and 2 wt%, of phosphorus brought by PO_xCR diluent. Thermal properties such as the temperature at 5% weight loss, the temperature at 50% weight loss, and the residue yield at 850 °C are summarized in Table 3. Firstly, the temperature at 5% weight loss ($T_{d,5\text{wt}\%}$) was similar for all the ARs, around 160 °C, and may be attributed to evaporation of residual solvent (i.e., xylene) trapped in the resin during crosslinking. Considering the temperature at 50% weight loss ($T_{d,50\text{wt}\%}$) the thermal stability was also similar for all the ARs (between 350 and 370 °C). Those results were similar to the values obtained in our previous study with the formulations containing PO_xCR and benzoic acid-based AR [28].

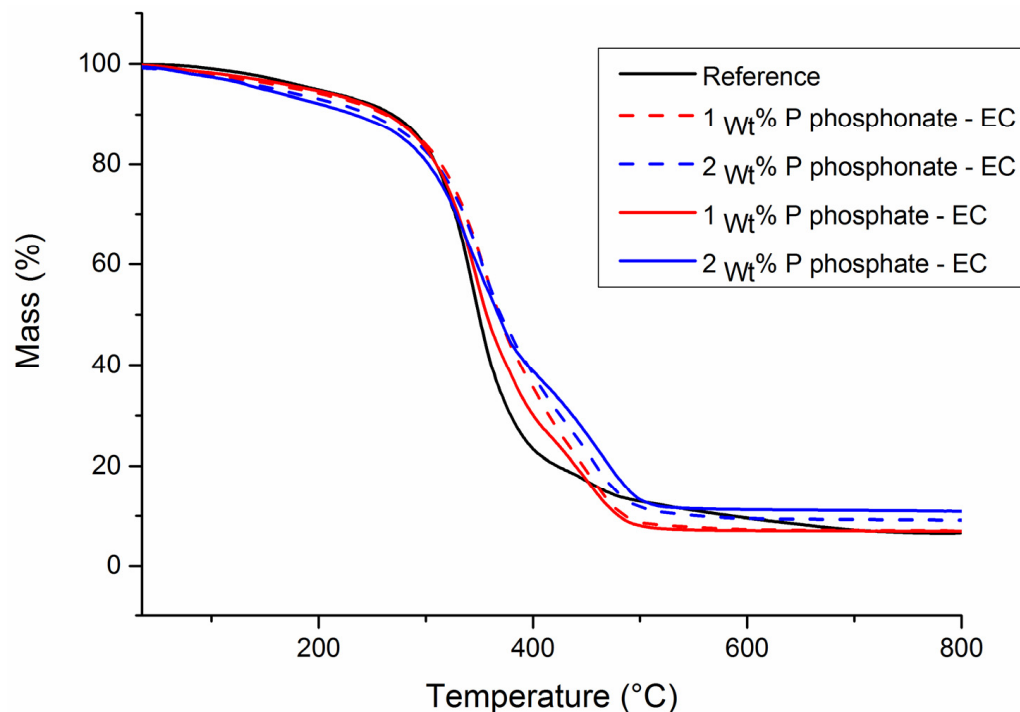


Figure 4. TGA thermograms of reference EC alkyd resin and PO_xCR diluent EC alkyd resins.

Table 3. Results of TGA analyses of reference EC alkyd resin and PO_xCR diluent EC alkyd resins.

<i>Reference</i>	<i>Phosphonate Monomer</i>	<i>Phosphonate</i>		<i>Phosphate Monomer</i>	<i>Phosphate</i>	
<i>wt% P</i>	0		1	2		1
$T_{d,5\%}$ ($^{\circ}\text{C}$)	165	294	164	161	350	163
$T_{d,50\%}$ ($^{\circ}\text{C}$)	350	448	360	370	462	368
Residue at $850\text{ }^{\circ}\text{C}$	6	6.4	7	9	16.5	7
						11

The oxidation degree of the phosphorus, and the increase amount of phosphorus in ARs only had a slight impact on the residue yield. At $850\text{ }^{\circ}\text{C}$, the char yield increased by 3% and 5% for the resins with, respectively, 2 wt% P brought by PO_3CR and PO_4CR , respectively, compared to the PO_xCR -free resin.

Numerous articles in the literature indicated that the char residue increases when the oxidation state of phosphorus increases [35–38]. Phosphonate and phosphate compounds act preferentially in the condensed phase by promoting char formation. Indeed, rearrangement and Diels–Alder reactions led to the formation of a carbon layer [39]. However, phosphonate compounds should be less efficient than phosphate compounds to promote char. In this study, the difference between phosphonate and phosphate cardanol was not significant.

Table 4 summarizes the data obtained from PCFC analyses. In standard conditions, combustion is complete in the PCFC test due to the excess of oxygen and the high combustor chamber ($900\text{ }^{\circ}\text{C}$). The total heat release (THR) and the peak of heat release rate (pHRR) are important characteristics to evaluate the flame-retardant (FR) properties of a material. Figure 5 exhibits the PCFC curves of the phosphorus cardanol-modified ARs. The increased amount of phosphorylated cardanol led to a reduction in pHRR and THR values, which demonstrated the FR properties of PO_3CR and PO_4CR diluents. The pHRR of the PO_xCR -free AR exhibited values of $206\text{ W}\cdot\text{g}^{-1}$ whereas the pHRR were $177\text{ W}\cdot\text{g}^{-1}$ for the ARs with 1 wt% P of PO_3CR and $168\text{ W}\cdot\text{g}^{-1}$ for the ARs with 1 wt% P of PO_4CR . The best results were obtained with the introduction of 2 wt% P of phosphate-cardanol, with a pHRR value of $119\text{ W}\cdot\text{g}^{-1}$. Those values are similar with the results obtained in our previous study with 3 wt% P PO_xCR . Thus, EC AR provided better thermal stability than AR containing acid benzoic. The temperatures of pHRR were similar for all the ARs, around $350\text{ }^{\circ}\text{C}$, which is consistent with TGA results. THR values slightly decreased with increasing amounts of PO_xCR diluent in ARs. Indeed, the THR value was decreased from $23.6\text{ KJ}\cdot\text{g}^{-1}$ for the PO_xCR -free AR to $21.5\text{ KJ}\cdot\text{g}^{-1}$ for the AR with 2 wt% P phosphate-cardanol. The energy of complete combustion (Δh) slightly decreased with the amount of phosphorylated cardanol. Furthermore, the residual content increased from 1% to 11% with, for 2 wt% P from PO_4CR . These results were in agreement with the TGA results and evidenced that phosphonate and phosphate compounds promoted char formation. Moreover, the residual content was slightly higher for the phosphate-cardanol, as already observed in TGA and in the previous study, evidencing that phosphate mainly acts in the condensed phase. The values of pHRR were slightly lower in this study than in the previously one with benzoic acid-based ARs [28]. Thus, results could indicate that formulations containing PO_xCR and EC-based ARs provided slightly better flame-retardant properties than formulations containing PO_xCR and acid benzoic-based ARs.

Table 4. Results of PCFC analyses of reference EC alkyd resin and PO_xCR diluent EC alkyd resins.

	<i>Reference</i>	<i>Phosphonate</i>		<i>Phosphate</i>	
<i>wt% P</i>	0	1	2	1	2
pHRR ($\text{W}\cdot\text{g}^{-1}$)	206	177	129	168	119
T at pHRR ($^{\circ}\text{C}$)	353	357	354	353	349
THR ($\text{KJ}\cdot\text{g}^{-1}$)	23.4	22.6	21.1	22.7	19.1
Residue content (%)	1	6	8	6	11
Δh ($\text{KJ}\cdot\text{g}^{-1}$)	23.6	24.0	23.4	24.1	21.5

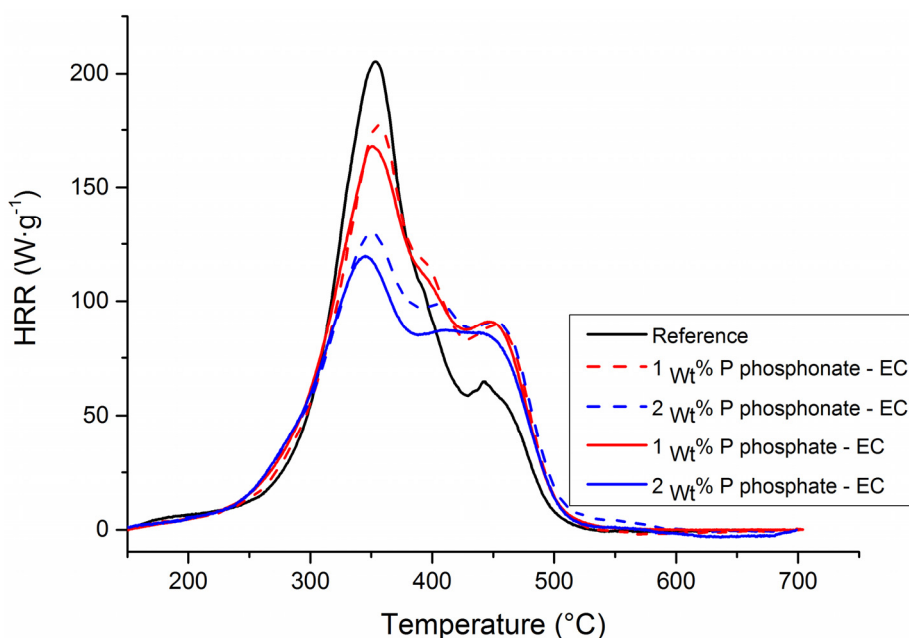


Figure 5. PCFC curves of reference EC alkyd resin and PO_xCR diluent EC alkyd resins.

The results demonstrated that the replacement of harmful volatile compounds by environmentally friendly phosphorus reactive diluents provided excellent thermal stability.

The cone calorimeter analyses allow studying the fire behavior of a material at bench-scale [40]. Cone calorimeter tests were performed with a heat flux of 35 kW·m⁻² under ventilated conditions. The results are summarized in Table 5. Figure 6 shows the cone calorimeter curves. Tests were performed on wood samples with 1 g of dry resin as a coating. Two pHRR can be observed, which is very common with wood samples. The first peak represents the heat release rate (pHRR₁) reached just after the ignition. After this first peak corresponding to the decomposition of the top surface of wood including the coating, the heat release rate decreases until reaching a plateau which corresponds to the steady-state decomposition rate. The lower the plateau, the slower the pyrolysis front progresses through the thickness of the wood. When the heat reaches the unexposed surface (insulated by rockwool), the heat is no longer evacuated, leading to a second peak of heat release rate (pHRR₂). This second peak of heat release rate is an artefact due to the geometry of the cone calorimeter test and is independent of the coating.

Table 5. Results of cone analyses of reference EC alkyd resin and PO_xCR diluent EC alkyd resins.

	Wood	Reference	Phosphonate		Phosphate	
wt% P	0	0	1	2	1	2
pHRR (kW·m ⁻²)	190 ± 10	295 ± 10	209 ± 11	182 ± 10	198 ± 8	172 ± 9
TTI (s)	65	10	25	25	41	40
THR (kJ·g ⁻¹)	9.4	9.9	8.9	8.4	8.7	8.2

Uncoated wood presents a moderate pHRR₁ at 190 KW·m⁻² and the PO_xCR-free AR led to a strong enhancement of the pHRR₁ (up to 295 kW·m⁻²). The use of a coating layer usually negatively affects the flame retardancy of wood but provides protection from external aggressions such as UV, weather and insects. The objective was to provide a coating with better flame retardancy than a standard coating. The introduction of PO₃CR and PO₄CR diluents had a strong influence on the pHRR₁ due to their ability to act in the condensed phase and to modify the decomposition pathway of the resin. Indeed, alkyd coatings with PO_xCR released the energy more slowly due to the modification of the degradation mechanism. Thereby, pHRR₁ decreased with the amount of phosphorylated cardanol.

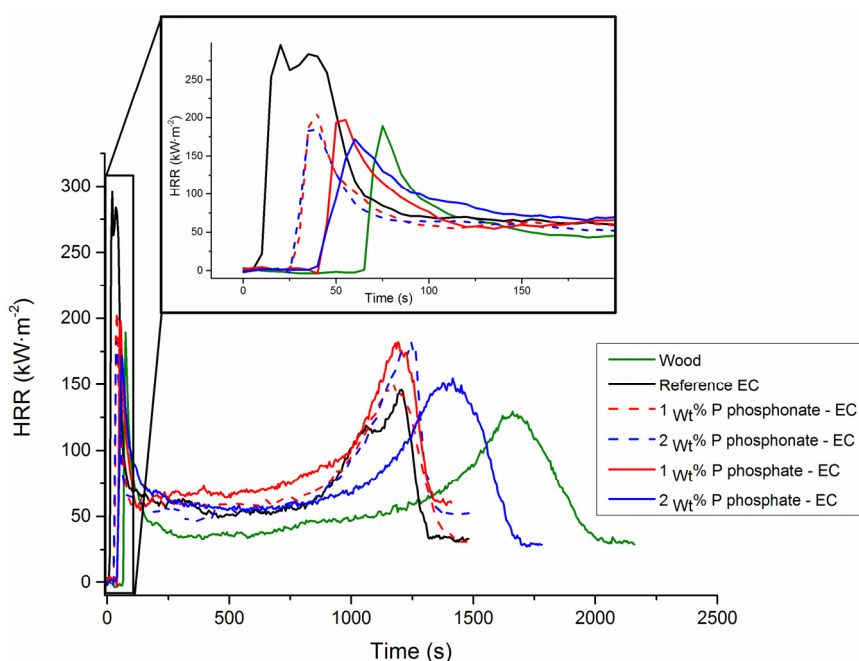


Figure 6. Cone calorimeter curves of reference EC alkyd resin and PO_xCR diluent EC alkyd resins.

The introduction of up to 2 wt% P PO₃CR has improved flame retardancy by decreasing the pHRR₁ from 295 kW·m⁻² to 182 kW·m⁻². The lowest pHRR for PO₄CR was obtained with 2 wt% P and exhibited a value of 172 kW·m⁻². Those results are similar with the results obtained in our previous study with PO₄CR at 3 wt% P. In this study, pHRR₁ decreased by almost 42% for the PO₄CR EC alkyd resin containing 2 wt% P compared to the PO_xCR-free AR. This result is slightly better than the one obtained in our previous study with benzoic AR containing PO₄CR at 2 wt% P (pHRR₁ decreased by 38% in our previous study) [28]. Once again, those results indicated that formulations containing PO_xCR and EC-based ARs provided better flame-retardant properties than formulations containing PO_xCR and benzoic acid-based ARs. Thereby, the replacement of benzoic acid by ethoxy cardanol had a positive influence on the reduction in pHRR₁ and reduced the use of petrosourced monomer. Furthermore, the difference between PO₃CR and PO₄CR was not significant with the cone calorimeter results. Time to ignition (TTI) is the time to achieve sustained flaming combustion at a particular external heat flux. TTI was increased with the introduction of phosphorylated cardanol. Nevertheless, TTI for all the woods with ARs was around two times lower than TTI for the uncoated wood. Indeed, the addition of alkyd coatings on the wood substrate reduced the TTI.

The charring from the resins cannot form a protective thick char able to prevent the heat diffusion into the wood. Therefore, total heat release (THR), final residue yield and effective heat of combustion (EHC) depend mainly on the wood and are not significantly influenced by the coating which impacts only pHRR₁ and time-to-ignition.

All those results confirmed the benefits provided by phosphorus cardanol reactive diluent on flame-retardant properties and the reduction in VOC amounts. Moreover, those results are consistent with the results obtained in our previous study.

3.3. Film Properties

Dry films with a thickness of 60 µm were obtained from the different resins with a film applicator. Adhesion, flexibility, gloss, drying time and chemical resistance have been determined and the results are presented in the following section in Tables 6 and 7.

Table 6. Adhesion, hardness, gloss and drying time of reference EC alkyd resin and PO_xCR diluent EC alkyd resins.

	<i>Reference</i>	<i>Phosphonate</i>	<i>Phosphate</i>	
<i>wt% P</i>	0	1	2	1
<i>Adhesion</i>	0	0	0	0
<i>Hardness (s)</i>	65	43	25	43
<i>Gloss 20°/60° (G.U.)</i>	68/95	64/98	70/98	64/97
<i>Drying time (min)</i>	75	190	350	190
<i>Color</i>	7	9	8	8

Table 7. Chemical resistances of reference EC alkyd resin and PO_xCR diluent EC alkyd resins.

	<i>Reference</i>	<i>Phosphonate</i>	<i>Phosphate</i>	
<i>wt% P</i>	0	1	2	1
<i>Water</i>	96 ± 1%	95 ± 1%	94 ± 2%	96 ± 2%
<i>HCl (0.1 M)</i>	78 ± 2%	80 ± 1%	77 ± 1%	79 ± 1%
<i>NaOH (0.1 M)</i>	70 ± 3%	69 ± 3%	70 ± 2%	68 ± 1%
<i>NaCl (5%)</i>	97 ± 4%	95 ± 2%	95 ± 3%	98 ± 2%

All the samples exhibited excellent adhesion properties. Indeed, the edges of the cuts were completely smooth and none of the squares of the grid were torn off. The results allowed an evaluation as class 0 according to ISO2409:2020. The introduction of PO_xCR in ARs did not impact the adhesion properties of the resins.

The hardness of the coating was impacted by the amount of phosphorylated cardanol introduced. The more flexible the film, the faster is the pendulum damped and therefore the less oscillations are required (one second corresponds to one oscillation of the pendulum). Indeed, the more flexible the film, the more it is able to absorb the energy of the pendulum. The number of oscillations decreased from 65 for the PO_xCR-free-AR to 25 for the resins with 2 wt% P phosphorylated cardanol. The introduction of phosphorylated cardanol in ARs provided more flexible films. Moreover, the flexibility increased with the amount of phosphorylated cardanol. Those results could be explained by the increasing amount of fatty chains with the increasing quantity of PO_xCR in formulations. These results are consistent with the *T_g* values with increasing the amount of phosphorylated cardanol in ARs. Nevertheless, even if the films were more flexible with phosphorylated cardanol, the values were close to that of the reference resin, which means that the films remained hard enough to allow the resin to maintain its film-forming properties for wood substrates.

The gloss of the coatings was firstly measured at 60° to determine the gloss level. All the ARs exhibited a high gloss level with values superior to 95 (between 95 and 98). The measurements were then studied at 20 °C. The reference resin showed a value of 65 and all the ARs containing PO_xCR exhibited values between 64 and 74. Thereby, those results demonstrated that the introduction of PO_xCR in formulations did not impact the gloss of the ARs.

The color of all the ARs was measured thanks to the Gardner color scale. The values are comprised between 1 and 18. The darker the color is, the higher the value. All the ARs exhibited similar values between 7 and 9, allowing them to be used for the same applications.

The introduction of phosphorylated cardanol as a reactive diluent in ARs increased the drying time. The drying time was increased by 2 h for the 1 wt% P-modified ARs compared to the drying time of PO_xCR-free AR. Moreover, the ARs with 2 wt% P showed the longest drying time, which was 5 h 50 min. Those results were expected because the proportion of ARs is lower in the formulations and the phosphorylated cardanol exhibited a low molecular weight and acted as a plasticizer by spacing the polymer chains. Thus, more covalent bonds had to be formed to create a crosslinking network. The PO_xCR-alkyd resins could be classified as medium oil length ARs as the introduction of PO_xCR increased the content of fatty chains. The drying time increased with the increasing amount of fatty chains [12]. Nevertheless, a drying time less than 6 h remained competitive with a drying

time of some commercial ARs with medium or long oil length. Those results are consistent with the results obtained in our previous study.

Table 7 presents the results of the determination of the chemical resistance of the resins. The higher the weight loss is, the lower the residual mass percentage and the less resistant the resin is to the solvent. The introduction of PO_xCR did not deteriorate the chemical resistance of the EC alkyd resins. Indeed, all the ARs containing phosphorylated cardanol exhibited similar chemical resistances to the PO_xCR -free AR. Moreover, ARs were highly resistant to NaCl solution with a residual mass higher than 95%. Nevertheless, the lower resistance to alkali solution can be due to hydrolysable ester groups in the ARs [31,41]. Indeed, saponification reactions could occur under those conditions.

4. Conclusions

In this article, benzoic acid used as a chain stopper for short oil alkyd resins synthesis has been replaced by a monofunctional cardanol (EC) and solvent has been replaced by flame-retardant PO_xCR reactive diluent, leading to an increase in the renewable carbon content by 23%. Phosphorylated cardanol compounds were grafted onto ARs after drying, which was demonstrated by GC content, ^1H HRMAS NMR and FTIR analysis. The introduction of phosphorylated cardanol as reactive diluent did not deteriorate the adhesion, nor the chemical resistance of ARs. Nevertheless, as expected, the drying time has increased and the T_g has decreased with the amount of phosphorylated cardanol introduced, but remained competitive. The fire behavior of those resins has been investigated by TGA, PCFC and cone calorimeter. The results obtained with TGA test were more similar in this study than in the previous one. Nevertheless, for PCFC and cone calorimeter analysis, formulations containing EC-based AR provided better flame-retardant properties than formulations containing acid benzoic-based AR. In this study, the ARs containing PO_xCR exhibited higher thermal stability than the PO_xCR -free AR. Phosphonate and phosphate-modified cardanol demonstrated similar results. Nevertheless, phosphate compounds exhibited higher char yield which could be attributed to the higher oxidation state of phosphorus, which promotes char formation and an action in the condensed phase. The best result was obtained with an AR modified with 2 wt% P phosphate cardanol and was slightly better than the one obtained in our previous study with benzoic AR containing 2 wt% P from PO_4CR . Finally, the 2 wt% P phosphate cardanol containing EC AR exhibited strong solvent reduction (50% compared to the PO_xCR -free alkyd resin) and high flame-retardant properties (reduction of 42% of pHRR in cone calorimeter analysis) while maintaining adequate film properties for wood application (drying time inferior to 7 h). Compared to the previous study, the replacement of benzoic acid by ethoxy cardanol has a positive influence on the flame-retardant properties and reduces the use of petrosourced monomer.

Supplementary Materials: The following supporting information can be downloaded at: <https://www.mdpi.com/article/10.3390/org4010009/s1>, 1. NMR spectra; 2. Standards.

Author Contributions: Conceptualization, M.D.; methodology, M.D.; software, M.D. and R.S.; validation, All; formal analysis, M.D., C.T. and R.S.; investigation, M.D., C.T. and R.S.; resources, D.L.B., S.C. and C.N.; data curation, M.D., C.T. and R.S.; writing—original draft preparation, M.D. and R.S.; writing—review and editing, All; visualization, M.D.; supervision, C.N. and S.C.; project administration, S.C. and C.N.; funding acquisition, D.L.B., S.C. and C.N. All authors have read and agreed to the published version of the manuscript.

Funding: This research received no external funding.

Data Availability Statement: Not applicable.

Acknowledgments: The authors would like to thank Lixol and especially Pierre Thouzeau and Line Maibeche for their contribution to the film properties analyses. The authors would like to thank CIRAM laboratory for the analysis of AMS radiocarbon.

Conflicts of Interest: The authors declare no conflict of interest.

References

1. Assanvo, E.F.; Gogoi, P.; Dolui, S.K.; Baruah, S.D. Synthesis, Characterization, and Performance Characteristics of Alkyd Resins Based on Ricinodendron Heudelotii Oil and Their Blending with Epoxy Resins. *Ind. Crops Prod.* **2015**, *65*, 293–302. [[CrossRef](#)]
2. Chiplunkar, P.P.; Pratap, A.P. Utilization of Sunflower Acid Oil for Synthesis of Alkyd Resin. *Prog. Org. Coat.* **2016**, *93*, 61–67. [[CrossRef](#)]
3. Chardon, F.; Denis, M.; Negrell, C.; Caillol, S. Hybrid Alkyds, the Glowing Route to Reach Cutting-Edge Properties? *Prog. Org. Coat.* **2021**, *151*, 106025. [[CrossRef](#)]
4. Kienle, R.H.; Rohlfs, H.C. Flexible Alkyd Resin and Method of Preparation. U.S. Patent 1,897,260, 14 February 1933.
5. Kienle, R.H.; Rohlfs, H.C. Flexible Alkyd Resin. CA Patent 347,682, 22 January 1935.
6. Hofland, A. Alkyd Resins: From down and out to Alive and Kicking. *Prog. Org. Coat.* **2012**, *73*, 274–282. [[CrossRef](#)]
7. La Nasa, J.; Degano, I.; Modugno, F.; Colombini, M.P. Alkyd Paints in Art: Characterization Using Integrated Mass Spectrometry. *Anal. Chim. Acta* **2013**, *797*, 64–80. [[CrossRef](#)] [[PubMed](#)]
8. Wicks, Z.W. Alkyd Resins. *Kirk-Othmer Encycl. Chem. Technol.* **2000**, *2*, 147–169.
9. Elliott, W.T. Alkyd Resins. *Surf. Coat.* **1993**, *5*, 76–109.
10. Ren, X.; Soucek, M. *Soya-Based Coatings and Adhesives*; American Chemical Society: New York, NY, USA, 2014; Volume 1178, pp. 207–254.
11. Mutar, M.A.; Abdul Hassan, N.M. Synthesis and Characterization of New Alkyd Resins (Short, Medium and Long) Based on Sunflower Oil and Linoleic Acid as Binder for Paints. *Int. J. Chem. Petrochim. Technol.* **2017**, *7*, 1–16.
12. Mustafa, S.F.M.; Gan, S.N.; Yahya, R. Synthesis and Characterization of Novel Alkyds Derived from Palm Oil Based Polyester Resin. *Asian J. Chem.* **2013**, *25*, 8737–8740. [[CrossRef](#)]
13. Hulsbosch, J.; Claes, L.; Jonckheere, D.; Mestach, D.; De Vos, D.E. Synthesis and Characterisation of Alkyd Resins with Glutamic Acid-Based Monomers. *RSC Adv.* **2018**, *8*, 8220–8227. [[CrossRef](#)] [[PubMed](#)]
14. Koning, C.; Lansbergen, A.; Koldijk, F.; Hendriks, H.; Papegaaij, A.; Smabers, R.; Buijsen, P.; Gehrels, C.; Reuvers, B.; Herrema, J. Novel Renewable Alkyd Resins Based on Imide Structures. *J. Coat. Technol. Res.* **2017**, *14*, 783–789. [[CrossRef](#)]
15. Denis, M.; Totée, C.; Le Borgne, D.; Caillol, S.; Negrell, C. Cardanol-Modified Alkyd Resins: Novel Route to Make Greener Alkyd Coatings. *Prog. Org. Coat.* **2022**, *172*, 107087. [[CrossRef](#)]
16. Li, W.S.J.; Cuminet, F.; Ladmíral, V.; Lacroix-Desmazes, P.; Caillol, S.; Negrell, C. Phosphonated and Methacrylated Biobased Cardanol Monomer: Synthesis, Characterization and Application. *Prog. Org. Coat.* **2021**, *153*, 106093. [[CrossRef](#)]
17. Le Parlement Européen et le Conseil de l’Union Européenne. Directice 2004/42/CE Du Parlement Européen et Du Conseil. *Off. J. Eur. Union* **2004**, *143*, 87–96.
18. Overbeek, A. Polymer Heterogeneity in Waterborne Coatings. *J. Coat. Technol. Res.* **2010**, *7*, 1–21. [[CrossRef](#)]
19. Nalawade, P.P.; Soucek, M.D. Modified Soybean Oil as a Reactive Diluent: Coating Performance. *J. Coat. Technol. Res.* **2015**, *12*, 1005–1021. [[CrossRef](#)]
20. Njuku, F.W.; Mwangi, P.M.; Thiong’o, G. Evaluation of Cardanol Acetate as a Reactive Diluent for Alkyd Coatings. *Int. J. Adv. Res.* **2014**, *2*, 928–941.
21. Jagtap, A.R.; More, A. Developments in Reactive Diluents: A Review. *Polym. Bull.* **2021**, *79*, 5667–5708. [[CrossRef](#)]
22. Jones, F.N. Alkyd Resins. *Ullman’s Encyclopedia Ind. Chem.* **2012**, *2*, 429–446.
23. Bora, M.M.; Deka, R.; Ahmed, N.; Kakati, D.K. Karanja, Seed Oil as a Renewable Raw Material for the Synthesis of Alkyd Resin. *Ind. Crops Prod.* **2014**, *61*, 106–114. [[CrossRef](#)]
24. Lee, R.; Grynnova, G.; Ingold, K.U.; Coote, M.L. Why are Sec-Alkylperoxy Bimolecular Self-Reactions Orders of Magnitude Faster than the Analogous Reactions of Tert-Alkylperoxyls? The Unanticipated Role of CH Hydrogen Bond Donation. *R. Soc. Chem.* **2016**, *18*, 23673–23679. [[CrossRef](#)]
25. Honzíček, J. Curing of Air-Drying Paints: A Critical Review. *Ind. Eng. Chem. Res.* **2019**, *58*, 12485–12505. [[CrossRef](#)]
26. Wang, H.; Zhang, C.; Zeng, W.; Zhou, Q. Making Alkyd Greener: Modified Cardanol as Bio-Based Reactive Diluents for Alkyd Coating. *Prog. Org. Coat.* **2019**, *135*, 281–290. [[CrossRef](#)]
27. Wang, H.; Zhang, C.; Zhou, Y.; Zhou, Q. Improvement of Corrosion Resistance and Solid Content of Zinc Phosphate Pigmented Alkyd Coating by Methacrylated Cardanol. *Mater. Today Commun.* **2020**, *24*, 101139. [[CrossRef](#)]
28. Denis, M.; Le Borgne, D.; Sonnier, R.; Caillol, S.; Totée, C.; Negrell, C. Phosphorus Modified Cardanol: A Greener Route to Reduce Volatile Organic Compounds and Impart Flame Retardant Properties to Alkyd Resin Coatings. *Molecules* **2022**, *27*, 4880. [[CrossRef](#)]
29. Laoutid, F.; Bonnaud, L.; Alexandre, M.; Lopez-Cuesta, J.M.; Dubois, P. New Prospects in Flame Retardant Polymer Materials: From Fundamentals to Nanocomposites. *Mater. Sci. Eng. R Rep.* **2009**, *63*, 100–125. [[CrossRef](#)]
30. Huggett, C. Estimation of Rate of Heat Release by Means of Oxygen Consumption Measurements. *Fire Mater.* **1980**, *4*, 61–65. [[CrossRef](#)]
31. Islam, M.R.; Beg, M.D.H.; Jamari, S.S. Alkyd Based Resin from Non-Drying Oil. *Procedia Eng.* **2014**, *90*, 78–88. [[CrossRef](#)]
32. Shao, X.; Su, L.; Zhang, J.; Tian, Z.; Zhang, N.; Wang, Y.; Wang, H.; Cui, X.; Hou, X.; Deng, T. Green Production of Phthalic Anhydride from Biobased Furan and Maleic Anhydride by an Acid Resin Catalyst. *ACS Sustain. Chem. Eng.* **2021**, *9*, 14385–14394. [[CrossRef](#)]
33. Carothers, W.H. Polymers and Polyfunctionality. *Trans. Faraday Soc.* **1936**, *32*, 39–49. [[CrossRef](#)]

34. Waitara, F.N. Evaluation of Cashew Nut Shell Liquid Based Products as Reactive Diluents for Alkyd Coatings. Ph.D. Thesis, Jomo Kenyatta University of Agriculture and Technology, Juja, Kenya, 2015.
35. Schartel, B. Phosphorus-Based Flame Retardancy Mechanisms—Old Hat or a Starting Point for Future Development? *Materials* **2010**, *3*, 4710–4745. [[CrossRef](#)]
36. Braun, U.; Balabanovich, A.I.; Schartel, B.; Knoll, U.; Artner, J.; Ciesielski, M.; Döring, M.; Perez, R.; Sandler, J.K.W.; Altstädt, V.; et al. Influence of the Oxidation State of Phosphorus on the Decomposition and Fire Behaviour of Flame-Retarded Epoxy Resin Composites. *Polymer* **2006**, *47*, 8495–8508. [[CrossRef](#)]
37. Velencoso, M.M.; Battig, A.; Markwart, J.C.; Schartel, B.; Wurm, F.R. Molecular Firefighting—How Modern Phosphorus Chemistry Can Help Solve the Flame Retardancy. *Angew. Chemie Int. Ed.* **2018**, *57*, 10450–10467. [[CrossRef](#)]
38. Horrocks, A.R.; Price, D. *Fire Retardant Materials*; Woodhead Publishing: Sawston, UK, 2001.
39. Green, J. A Review of Phosphorus-Containing Flame Retardants. *J. Fire Sci.* **1996**, *14*, 353–366. [[CrossRef](#)]
40. Qi, J.; Wen, Q.; Zhu, W. Research Progress on Flame-Retarded Silicone Rubber. *Conf. Ser. Mater. Sci. Eng.* **2018**, *392*, 032007. [[CrossRef](#)]
41. Ikhuoria, E.U.; Aigbodion, A.I.; Okieimen, F.E. Enhancing the Quality of Alkyd Resins Using Methyl Esters of Rubber Seed Oil. *Trop. J. Pharm. Res.* **2003**, *3*, 311. [[CrossRef](#)]

Disclaimer/Publisher’s Note: The statements, opinions and data contained in all publications are solely those of the individual author(s) and contributor(s) and not of MDPI and/or the editor(s). MDPI and/or the editor(s) disclaim responsibility for any injury to people or property resulting from any ideas, methods, instructions or products referred to in the content.